

Seismic Retrofit of Bridge Steel Truss Piers Using a Controlled Rocking Approach

Michael Pollino¹ and Michel Bruneau²

Abstract: This paper investigates a seismic retrofit technique that allows bridge steel truss piers to uplift and rock on their foundation. Displacement-based passive energy dissipation devices (buckling-restrained braces, or BRBs) are implemented at the uplifting location to control the rocking response while providing additional energy dissipation. The hysteretic behavior of the controlled rocking system is developed for a static cyclic load applied to the top of a bridge pier, representing the dominant mode of vibration. Some existing methods of analysis are considered in predicting the response of the controlled rocking system in terms of maximum displacements. A capacity-based design procedure is established for sizing the BRBs and a design example provided to illustrate the key steps. Methods to predict design response values (displacements, velocity, forces) are discussed, and a parametric study, based on nonlinear time history analysis, is performed to verify the effectiveness of these methods. The parameters in the study include the pier aspect ratio (h/d), the local strength ratio (η_L) and an effective period of vibration (T_{eff}). Results of the study are presented as normalized by the design response values and are shown, in almost all cases, to be conservative.

DOI: 10.1061/(ASCE)1084-0702(2007)12:5(600)

CE Database subject headings: Bridge piers; Bridges, steel; Seismic effects; Retrofitting; Energy dissipation; Trusses.

Introduction

Recent earthquakes, such as the 1989 Loma Prieta, 1994 Northridge, and 1995 Kobe earthquakes, have demonstrated the need for improved methods for the design and construction of highway bridges to withstand seismic force and displacement demands. Span collapses or significant damage from those earthquakes (particularly Kobe) have left many large lifeline bridges unusable until repairs were made, contributing to substantial losses to the local economy. Highway bridges deemed critical in the response and recovery efforts following a major earthquake (also known as lifeline bridges) need to remain operational after an earthquake, requiring the bridge to respond in a mostly elastic manner with little to no residual displacements.

Steel truss bridge piers supporting a slab-on-girder or truss bridge exist in nearly every region of the United States. Lateral load-resisting pier elements consisting of built-up lattice-type members with riveted connections were prevalent at the time of construction of many of these bridges. These built-up lattice-type members can suffer global and local buckling, resulting in loss of pier lateral strength and major structural damage during an earthquake (Lee and Bruneau 2004). Furthermore, existing riv-

eted connections and deck diaphragm bracing members typically possess little to no ductility (Ritchie et al. 1999). Another possible nonductile failure location is the anchorage connection at the pier-to-foundation interface.

While strengthening these existing vulnerable elements to resist seismic demands elastically is an option, this method can be expensive and also gives no assurance of performance beyond the elastic limit. Therefore, it is desirable to have structures able to deform inelastically, limiting damage to easily replaceable ductile structural “fuses,” able to produce stable hysteretic behavior while protecting existing nonductile elements. Ideally, it would also be desirable to prevent residual inelastic deformations and have structural systems that can be self-centering following an earthquake.

Releasing of the pier-to-foundation anchorage connections’ tensile capacity (or allowing them to fail) would enable a steel truss pier to rock on its foundation, effectively increasing its period and partially isolating the pier. Adding passive energy dissipation devices at the uplifting location would restrain the uplift displacements while providing additional energy dissipation. This retrofit strategy also is advantageous because the location of the pier anchorage tends to be easily accessible compared to other parts of the bridge. The rocking system described has an inherent restoring force, capable of allowing for automatic recentering of the tower, leaving the bridge with no residual displacements after an earthquake. A sketch of such a retrofitted bridge pier is shown in Fig. 1.

The rocking of structures during earthquake excitation has been observed in the past and was first investigated by Housner (1963), who considered the response of rigid blocks. Meek (1975) introduced aspects of structural flexibility to the seismic response of single-degree-of-freedom (SDOF) rocking structures. The use of rocking structural systems for the seismic design and retrofit of structures has been examined analytically and experimentally by Kelley and Tsztoo (1977), Priestley et al. (1978), Mander and

¹Ph.D. Candidate, Dept. of Civil, Structural, and Environmental Engineering, Univ. at Buffalo, Buffalo, NY 14260. E-mail: mpollino@eng.buffalo.edu

²Director, MCEER, and Professor, Dept. of Civil, Structural and Environmental Engineering, Univ. at Buffalo, Buffalo, NY 14260. E-mail: bruneau@buffalo.edu

Note. Discussion open until February 1, 2008. Separate discussions must be submitted for individual papers. To extend the closing date by one month, a written request must be filed with the ASCE Managing Editor. The manuscript for this paper was submitted for review and possible publication on March 4, 2005; approved on September 18, 2006. This paper is part of the *Journal of Bridge Engineering*, Vol. 12, No. 5, September 1, 2007. ©ASCE, ISSN 1084-0702/2007/5-600-610/\$25.00.

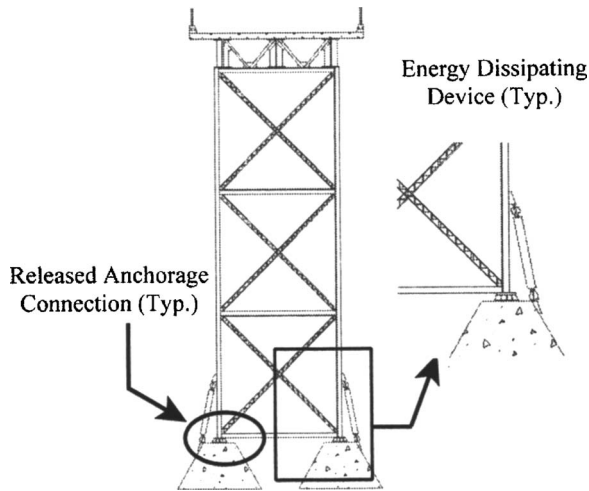


Fig. 1. Retrofitted bridge steel truss pier using controlled rocking approach

Cheng (1997), Toranzo et al. (2001), and Midorikawa et al. (2003).

A rocking bridge pier concept has been implemented or considered for the seismic design or retrofit of a few bridges. The South Rangitikei Rail Bridge, located in Mangaweka, New Zealand, was designed and constructed in the 1970s with pier legs allowed to uplift under seismic loads (Priestley et al. 1996). Torsional steel yielding devices were added to control the amount of uplift. The North Approach of the Lions' Gate Bridge, located in Vancouver, British Columbia, was retrofitted using a rocking bridge pier approach (Dowdell and Hamersley 2000). Flexural yielding steel devices were placed at the anchorage interface to provide hysteretic damping and limit the uplifting displacements. Other bridges that allow rocking (or at least partial uplift of pier legs) as a means of seismic resistance include the Carquinez Bridge (Jones et al. 1997) and the Golden Gate Bridge (Ingham et al. 1995), both of which are located in California.

While many types of energy dissipation devices exist, the device considered here is the buckling-restrained brace (unbonded brace, or BRB). A BRB consists of a steel core surrounded by a buckling restraining part, allowing the brace to reach full yield in tension and compression. The component and system behavior of BRBs has been evaluated by Watanabe et al. (1988), Wada et al. (1989), Watanabe and Nakamura (1992), Hasegawa et al. (1999), Iwata et al. (2000), and Black et al. (2002).

This paper describes the static hysteretic cyclic response of the proposed controlled rocking system for the seismic retrofit of bridge steel truss piers and investigates existing simple methods of analysis for predicting the response of the system in terms of maximum developed displacements. A capacity-based design procedure is developed for sizing the BRBs such that response meets a set of design constraints, and an example is presented to illustrate the design process. A parametric study, based on nonlinear inelastic time history analysis, is performed to investigate system performance and assess the simplified methods of analysis for predicting the design response values.

Hysteretic Response of Controlled Rocking Bridge Pier System

The key parameters for the static cyclic hysteretic response of the controlled rocking bridge pier system considered here include

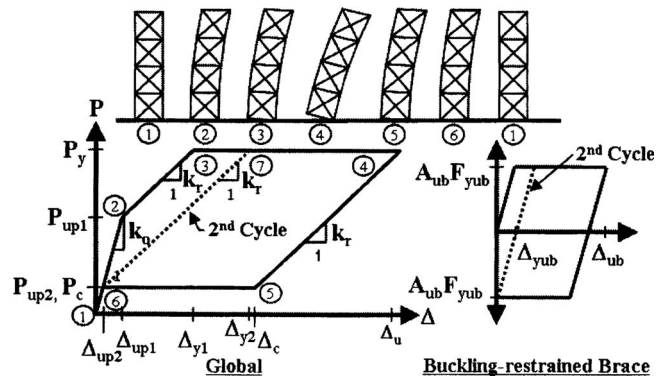


Fig. 2. Cyclic pushover of controlled rocking bridge pier and buckling-restrained brace behavior

the fixed-base lateral stiffness of the existing steel truss pier (k_o), the height-over-width aspect ratio of the pier (h/d), and the cross-sectional area, effective length, and yield stress of the BRB (A_{ub}, L_{ub}, F_{yub}). Identical BRBs implemented at the base are considered here to behave elastoplastically and are assumed to be implemented vertically such that they do not transfer horizontal shear at the base of the pier. Also, the weight excited by horizontally imposed accelerations (w_h) and the vertical gravity weight carried by a pier (w_v) are assumed equal and expressed as w .

The model considers motion of the pier in a direction orthogonal to the bridge deck and assumes no interaction with other piers or abutments through the bridge deck. The response of an actual bridge must consider behavior of the entire bridge system in the longitudinal and transverse directions, including each pier's and abutment's properties, bridge deck properties, and the connection details between the deck and piers. However, this will vary significantly from bridge to bridge, and the purpose of this study was to evaluate the behavior of such a controlled rocking pier as a component of an entire bridge system. Also, the existing anchorage connection is assumed to provide no resistance to vertical movement but is able to transfer the horizontal base shear.

The various steps and physical behaviors that develop through a typical half-cycle are shown in Fig. 2. By symmetry, the process repeats itself for movement in the other direction. Transition from first to second-cycle response occurs when the BRBs yield in compression and the braces carry a portion of the weight after the system comes to rest upon completion of the cycle (a phenomenon explained later).

First-Cycle Response

The horizontal load applied at the top of the pier, P , as a function of the lateral displacement, Δ , before uplift begins, consists of the elastic stiffness of the pier's structural members, defined by

$$P = k_o \Delta \quad (1)$$

Uplifting of a tower leg begins when the restoring moment created by the tributary vertical bridge weight is overcome by the applied moment (Position 2 in Fig. 2). The horizontal force at the point of uplift during the first cycle is defined by

$$P_{up1} = \frac{w}{2} \left(\frac{d}{h} \right) \quad (2)$$

and the displacement at the point of uplift in the first cycle is defined by

$$\Delta_{up1} = P_{up1}/k_o \quad (3)$$

After uplift, the BRB attached to the uplifting leg is activated. The global stiffness is reduced and becomes a function of the pier's lateral stiffness, k_o , and the uplifting BRB's contribution to the horizontal stiffness. The structural stiffness from uplift to the yield point (Steps 2 to 3 in Fig. 2) is defined here as the elastic rocking stiffness and is expressed by

$$k_r = \left(\frac{1}{k_o} + \frac{1}{\frac{EA_{ub}}{L_{ub}} \left(\frac{d}{h} \right)^2} \right)^{-1} \quad (4)$$

The horizontal force at the onset of brace yielding, P_y , and thus the structural system yield strength is defined by

$$P_y = \left(\frac{w}{2} + A_{ub}F_{yub} \right) \frac{d}{h} = \frac{w d}{2 h} \cdot (1 + \eta_L) \quad (5)$$

where η_L is defined here as the system's local strength ratio equal to

$$\eta_L = \frac{A_{ub}F_{yub}}{w/2} \quad (6)$$

The corresponding system yield displacement for the first cycle, Δ_{y1} , is defined as

$$\Delta_{y1} = \left(\frac{w}{2k_o} + \frac{A_{ub}F_{yub}}{k_r} \right) \frac{d}{h} = \frac{w d}{2 h} \cdot \left(\frac{1}{k_o} + \frac{\eta_L}{k_r} \right) \quad (7)$$

Ignoring strain hardening in the brace and any second-order effects, the system has zero postelastic stiffness and is deformed to its ultimate displacement (Δ_u). Methods of predicting the system's ultimate displacement will be discussed later.

As the horizontal load is reduced, the pier first responds elastically with stiffness k_r , and the tensile force in the BRB reduces per its initial elastic properties. The applied lateral load at the top of the pier at the point of compressive yielding of the brace (Point 5 in Fig. 2) is defined by

$$P_c = \left(\frac{w}{2} - A_{ub}F_{yub} \right) \left(\frac{d}{h} \right) = \frac{w d}{2 h} (1 - \eta_L) \quad (8)$$

The corresponding displacement at this point is defined as

$$\Delta_c = \Delta_u - \frac{2A_{ub}F_{yub} \frac{d}{h}}{k_o} - 2 \frac{F_{yub}L_{ub} \frac{h}{d}}{E} \quad (9)$$

The BRB displaces plastically in compression and again is assumed to yield with no significant stiffness until the uplifted pier leg returns in contact to its support (Steps 5 to 6 in Fig. 2). At this point of contact, the system stiffness is again defined by k_o .

Second-Cycle Response

As a BRB yields in compression and the pier settles back to its support, the BRB effectively carries a portion of the bridge weight equal to its compressive capacity (assumed to be $A_{ub}F_{yub}$). As a result of this transfer of the gravity load path (now partially through the BRBs), a smaller horizontal force is required to initiate uplift, causing an earlier transition from stiffness k_o to the rocking stiffness k_r , thus increasing the flexibility and system yield displacement from the first-cycle response, as can be seen by the second-cycle curve in Fig. 2.

The horizontal force at the onset of uplift can be shown equal to P_c [defined by Eq. (8)] and is defined for the second and subsequent cycles as

$$P_{up2} = P_c = (1 - \eta_L) \frac{w d}{2 h} < P_{up1} \quad (10)$$

The yield displacement can be expressed as

$$\Delta_{y2} = \frac{w d}{2 h} \cdot \left(\frac{1 - \eta_L}{k_o} + \frac{2\eta_L}{k_r} \right) > \Delta_{y1} \quad (11)$$

The yield strength of the system, P_y , is unchanged. The force in the BRB changes from its compressive strength ($A_{ub}F_{yub}$) to tension yielding ($A_{ub}F_{yub}$) for the second and subsequent cycles that exceed deck level displacement of Δ_{y2} . Note that the controlled rocking bridge pier system considered develops a flag-shaped hysteresis. This is due to the combination of pure rocking response from the restoring moment, provided by the bridge deck weight, and energy dissipation provided by yielding of the BRBs.

Influence of Second-Order Effects on Hysteretic Response

The restoring moment, M_r , for base rocking is provided by gravity. As the center of mass displaces, this restoring moment reduces as a function of the horizontal seismically induced displacement of the bridge deck such that

$$M_r(\Delta_i) = w \left(\frac{d}{2} - \Delta_i \right) \quad (12)$$

This loss in restoring moment can be written in terms of the loss in horizontal base shear as

$$P_r(\Delta_i) = \frac{w}{h} \left(\frac{d}{2} - \Delta_i \right) = \frac{w d}{2 h} - \frac{w}{h} \Delta_i = P_{up1} - \frac{w}{h} \Delta_i \quad (13)$$

Considering this effect along with the strain hardening of the BRB, in the form of a postyield stiffness ratio (α_{ub}), results in a global postyield stiffness of

$$k_{py} = \alpha_{ub} k_{ub} \left(\frac{d}{h} \right)^2 - \frac{w}{h} \quad (14)$$

Generally, the effect of the strain hardening of the BRB is greater than the effective negative stiffness due to the nonlinear geometric effect, thus resulting in a positive global postyield stiffness, k_{py} . For the pier widths and aspect ratios considered herein (representing bridge piers), a modestly sized BRB can result in a positive global postyield stiffness. The methods of analysis proposed in this paper for determining the maximum displacement response of the controlled rocking system do not take into account second-order effects, assuming they are negligible.

Methods of Analysis Considered for Determining Maximum Pier Displacements

Methods for predicting system displacement response based on equal displacement and equal energy theory (Newmark and Hall 1982) have been used with reasonable confidence for well-detailed steel seismic lateral force resisting systems such as moment resisting frames (MRFs), eccentrically braced frames (EBFs), and concentrically braced frames (CBFs). However, the effectiveness of these methods with the flag-shaped hysteretic be-

havior considered here is unknown. Therefore, a few simplified analysis methods are investigated analytically as part of the parametric study (presented later) for their effectiveness in predicting the seismic response of a controlled rocking system in terms of maximum displacements that can be used later in the design process of the controlled rocking approach.

The first analysis method considered consists of characterizing system response in a manner similar to the nonlinear static procedure (NSP) described in FEMA 356 (FEMA 2000), while a second is similar to the nonlinear static procedure for passive energy dissipation systems found in FEMA 274 (FEMA 1997). The first method is typically used for MRFs, EBFs, and CBFs, while an analysis procedure similar to the second can be found in the NCHRP 12-49 document (ATC/MCEER 2003). Each of these procedures is described in its respective documents; thus only the important parameters from these procedures related to the behavior of the controlled rocking system are discussed here.

Method 1

The procedure described in the FEMA 356 document relies on the calculation of an effective period of vibration, a series of factors, and a design spectrum to calculate maximum displacements. Assuming that the hysteretic behavior is stable, without strength or stiffness degradation; that P - Δ effects are not significant; and that the system's effective period lies in the long period range, then each of the factors is set to unity and the effective period of vibration is the key parameter. This effective period of vibration, T_{eff} , is defined as

$$T_{\text{eff}} = 2\pi \sqrt{\frac{m}{k_{\text{eff}}}} \quad (15)$$

A characterization of the effective stiffness similar to that in FEMA 356 for systems that experience progressive yielding and do not have a definite yield point is used here and defined as

$$k_{\text{eff}} = k_o \left(\frac{\Delta_{up2}}{\Delta_{y2}} \right) + k_r \left(\frac{\Delta_{y2} - \Delta_{up2}}{\Delta_{y2}} \right) \quad (16)$$

where all terms have been defined previously. The effective stiffness could also simply be taken as the rocking stiffness, k_r , [Eq. (4)], which represents a lower bound of Eq. (16), thus resulting in an upper bound in the predicted displacement using this method.

Method 2

The method proposed in the FEMA 274 document for the design of passive energy dissipation systems uses spectral capacity (pushover) and demand curves. Conversion of the demand and capacity (pushover) curve to spectral ordinates is based on modal analysis theory. The bridge piers are assumed here to behave as a single degree of freedom system representing the dominant horizontal mode of vibration. The added energy dissipation from the BRBs is converted to equivalent viscous damping and the seismic demand curve reduced from the 2% damped spectrum. For the flag-shaped hysteretic behavior of the controlled rocking system, the equivalent viscous damping can be determined by

$$\xi_{\text{eff}} = \xi_o + \xi_{\text{hys}} \quad (17)$$

where ξ_o = inherent structural damping (assumed to be 2%) and ξ_{hys} = hysteretic damping provided by BRBs during rocking response. The hysteretic damping can be approximated by modify-

ing the equivalent damping of a bilinear system (with no strain hardening) by a factor q

$$\xi_{\text{hys}} = q \cdot \xi_{bi} = \frac{\eta_L}{1 + \eta_L} \cdot \frac{2}{\pi} \cdot \left(1 - \frac{\Delta_{y2}}{\Delta_u} \right) \quad (18)$$

Factors for reducing the spectrum for the added energy dissipation are given in FEMA 274.

The effectiveness of these methods is presented following the sections on design as part of the parametric study, and the steps of Method 2 are presented in detail as part of the design example.

Design Constraints for the Controlled Rocking Approach

To ensure satisfactory seismic performance of this retrofit approach, a number of design constraints must be identified and a systematic design procedure formulated following capacity-based design principles. Specific design constraints include: (1) pier drift limits; (2) ductility demands on the steel yielding devices; (3) limits to allow for pier self-centering; and (4) maximum developed dynamic forces within the pier and foundation (capacity protection). Methods of determining response values for design (design response values) are introduced along with each constraint.

Pier Drift

For the purpose of this study and to illustrate how such limits would be considered, two displacement limits are arbitrarily imposed here, to prevent excessive P - Δ effects on seismic behavior, and system overturning instability. Additional limits can be added on a case-by-case basis, as necessary.

A requirement shown to limit P - Δ effects based on the dynamic analysis of SDOF systems with various hysteretic relationships is taken from the *Recommended LRFD Guidelines for the Seismic Design of Highway Bridges* (ATC/MCEER 2003). The limit is given by

$$\Delta_{u1} \leq 0.25 \frac{P_y}{w} h \quad (19)$$

where w = horizontal reactive weight of the bridge tributary to the pier, h = pier height, and P_y = lateral strength of the pier defined by Eq. (5).

The limit to ensure stability against overturning is based on preventing displacement of the center of mass from exceeding half of the base width ($d/2$) with a large factor of safety such that

$$\Delta_{u2} \leq \frac{d}{2FS} \quad (20)$$

A factor of safety (FS) of 5 is conservatively recommended. The methods of analysis presented previously are used to determine maximum developed displacements. Both displacement constraints can typically be satisfied by increasing A_{ub} and/or decreasing L_{ub} .

Ductility Demands on Buckling-Restrained Brace

Limits on the inelastic strain demands of BRBs are set to ensure that they behave in a stable, predictable manner. These limits should be based on engineering judgment and experimental test data on the ultimate inelastic cyclic response of such braces. An

the dynamic effects to be in-phase. Assuming elastic response of pier members (consistent with the design objectives), the total force in the leg can be written as

$$P_{uL} = P_{vo} + P_{wL} + P_{uw} \quad (27)$$

where P_{vo} = maximum force developed due to the vertical velocity of the pier leg upon impact, P_{wL} = force developed in the leg due to its tributary gravity weight, including dynamic amplification, and P_{uw} = force developed in the leg at the first-tier level of the pier, caused by the horizontal base shear transferred through the pier diagonals (Fig. 3). The total force developed in a pier leg is taken here as equal to

$$P_{uL} = v_o \sqrt{\frac{m \cdot k_L}{2}} + R_{dL} \cdot \frac{w}{2} + \left(\frac{w}{2} + A_{ub} F_{yub} \right) \cdot R_{dv} \cdot \left(1 - \frac{d}{2h} \right) \quad (28)$$

where v_o = impact velocity of the pier leg, k_L = axial stiffness of a pier leg, and R_{dL} = amplification factor for the tributary gravity weight of the impacted pier leg. Summation of all dynamic demands may lead to overly conservative predictions, and an SRSS or CQC combination rule applied to the dynamic effects may be more appropriate.

From the perspective of seismic retrofit, the BRB strength, $A_{ub} F_{yub}$, and the impact velocity, v_o , are the primary parameters influencing demands on the pier legs. Protection of these elements depends on both A_{ub} and v_o . Assuming that a value of A_{ub} is established during the design process to satisfy the effective lateral base shear limit [Eq. (26)] or the self-centering limit [Eq. (24)], the limiting impact velocity can be written as

$$v_{o,allow} = \frac{P_{uL,allow} - R_{dL} \cdot \frac{w}{2} - \left(\frac{w}{2} + A_{ub} F_{yub} \right) \cdot R_{dv} \cdot \left(1 - \frac{d}{2h} \right)}{\sqrt{\frac{m \cdot k_L}{2}}} \quad (29)$$

where $P_{uL,allow}$ = maximum allowable force, controlled by either the strength of the pier leg or foundation. Other limits may need to be defined to prevent foundation settlement and/or other serviceability requirements. Limiting v_o is typically achieved by increasing A_{ub} and decreasing L_{ub} ; however, increasing the allowable impact velocity of the pier leg, $v_{o,allow}$, is most effectively done by decreasing A_{ub} . For design purposes, the maximum impact velocity could simply be determined from the inelastic pseudovelocity such that

$$v_o = PS_{vi} \cdot \frac{d}{h} \quad (30)$$

Systematic Design Procedure

To achieve the desired ductile performance of a retrofitted rocking steel truss bridge pier, the BRBs must be proportioned to meet the relevant design constraints. The key steps of the design procedure are described briefly below

1. Establish seismic demand parameters to construct the design response spectrum based on site location, soil properties, etc., following ATC/MCEER (2003).
2. Determine relevant existing pier properties. These values include the pier aspect ratio (h/d), the "fixed-base" lateral

stiffness of the pier (k_o), the axial stiffness of a pier leg (k_L), and the horizontal and vertical tributary reactive weights for the given pier, w_h and w_v , respectively. The dynamic amplification factors, R_{dv} and R_{dL} , can be determined using methods presented in Pollino and Bruneau (2004). Also, the lateral strength of the pier ($P_{u,allow}$) and capacity of the pier legs ($P_{uL,allow}$) need to be determined.

3. Ensure that pier uplifting and rocking motion will be initiated for the design seismic demand. First, determine the spectral acceleration value for the fixed-base pier. If the pier's period of vibration, T_o , is greater than the characteristic period of the spectrum, T_s (defined in ATC/MCEER 2003), then the elastic spectral acceleration for the fixed-base pier is given by

$$S_{a,fixed} = \frac{S_{D1} \cdot s}{B_L \cdot T_o} \quad (31)$$

Using the spectral acceleration value given by Eq. (31), pier uplifting and rocking motion will be initiated if the following statement is true:

$$\frac{S_{a,fixed}}{g} \geq \frac{1}{2} \frac{w_v d}{w_h h} \quad (32)$$

If this statement is not true, then uplift will not occur for the given seismic demand. In fact, the value on the left side of the equation should be much greater (>2) than the right side for the rocking approach to be effective. If not, the pier is likely to be relatively squat, and another retrofit approach would likely be more effective (Berman and Bruneau 2005).

4. Establish limits set by the pier drift, self-centering, and effective lateral base shear constraints, Eqs. (19), (20), (24), and (26) respectively, since these limits are independent of A_{ub} or L_{ub} .
5. Begin sizing of BRBs by assigning a yield force to the braces ($A_{ub} F_{yub}$) to satisfy the effective lateral base shear constraint [Eq. (26)]. If no BRB area can satisfy this constraint, partial pier strengthening may be required.
6. Design L_{ub} to satisfy the ductility demand constraint [Eq. (23)]. An initial effective length can be determined by estimating the uplifting displacement [from Eq. (22)] such that

$$L_{ubo} = \frac{\Delta_{uplift,o}}{0.015} = \frac{\left[\frac{S_{D1} T_{effo} \cdot s}{4\pi^2} - \frac{\frac{w d}{2 h} \cdot (1 + \eta_L)}{k_o} \right] \cdot \frac{d}{h}}{0.015} \quad (33)$$

with the initial effective period of vibration, T_{effo} , set equal to $1.2T_o$.

7. Establish limits set by the BRB ductility demand and pier leg demand constraints, Eqs. (23) and (29), using the previous iteration's brace dimensions.
8. Analyze response of the retrofitted system with the initially sized BRB using a simplified analysis method to determine the design displacement response.
9. Evaluate the design velocity response and determine if all constraints defined in Steps 4 and 7 are satisfied.
10. Modify the BRB dimensions, as necessary, to satisfy constraints. Guidance on varying brace dimensions to satisfy each constraint was provided in the constraints section.

Table 1. Controlled Rocking System Example

Design iteration	0	1	2		Units
A_{ub}	2,000	2,000	1,500	—	mm ²
L_{ub}	1,900	1,900	2,750	—	mm
Constraints					
Δ_{u1} [Eq. (19)]	914	914	914	—	mm
Δ_{u2} [Eq. (20)]	732	732	732	—	mm
Δ_{uplift} [Eq. (22)]	28.5	28.5	41.3	—	mm
A_{ub4} [Eq. (26)]	2,926	2,926	2,926	—	mm ²
$v_{o,allow}$ [Eq. (29)]	118	118	156	—	mm/s
A_{ub3} [Eq. (24)]	3,681	3,681	3,681	—	mm ²
Design response values			TH analysis		
Δ_u (Fig. 5)	138	158	188	187	mm
Δ_{uplift} [Eq. (22)]	28.4	32.9	41.0	40.1	mm
v_o [Eq. (30)]	—	137	143	141	mm/s
P_u [Eq. (25)]	—	—	487	379	kN
$P_{u,L}$ [Eq. (28)]	—	—	3,920	2,262	kN

Graphical Design Procedure

As has been shown, the design of retrofitted bridge piers using the controlled rocking approach requires that a number of design constraints be met to achieve the desired performance. To assist in the design process, a visual aid is proposed to illustrate the ranges of compliance and noncompliance of the design constraints as a function of two key design parameters. The constraints are expressed as boundaries enclosing a solution space where all constraints are satisfied, and thus a range of design solutions can be found.

A similar approach has been proposed by Sarraf and Bruneau (1998). The two key design parameters used here are A_{ub} and L_{ub} . Each boundary line is defined with A_{ub} as a function of L_{ub} . In some cases the constraint boundary lines can be simply defined algebraically, such as the effective lateral base shear [Eq. (26)] and self-centering limit [Eq. (24)] constraints. However, all other constraints are dependent on the ultimate deck-level displacement, Δ_u , which itself is dependent on A_{ub} and L_{ub} and is determined using analysis Method 2; Δ_u cannot be defined algebraically in terms of A_{ub} and L_{ub} , but it can be determined iteratively for each pair of design parameters. The graphical procedure will be presented, along with the step-by-step approach presented previously, in the design example.

Example

To illustrate the above-proposed design procedure, a bridge is assumed to be located on site class B and the site coefficients, F_a and F_v are equal to 1. The seismic demand is obtained from a design spectrum specified in ATC/MCEER (2003) with one-second (S_1) and short-period (S_s) spectral acceleration values of 0.5 and 1.25g, respectively, corresponding to 5% damping. This leads to a characteristic spectral period, T_s , of 0.4 s, typical of a rock site.

The example uses a pier with an aspect ratio of 4 ($h=29.26$ m, $d=7.32$ m) with horizontal and vertical tributary weights (w_h and w_v) equal to 1730 kN. The pier lateral stiffness (k_o) is taken as 12.6 kN/mm, and thus the fixed-base period of vibration (T_o) is equal to 0.74 s. Also, the axial stiffness of a pier leg is taken to be 212 kN/mm, and the lateral strength of the pier ($P_{u,allow}$) and capacity of a pier leg ($P_{uL,allow}$) is taken as 605 and

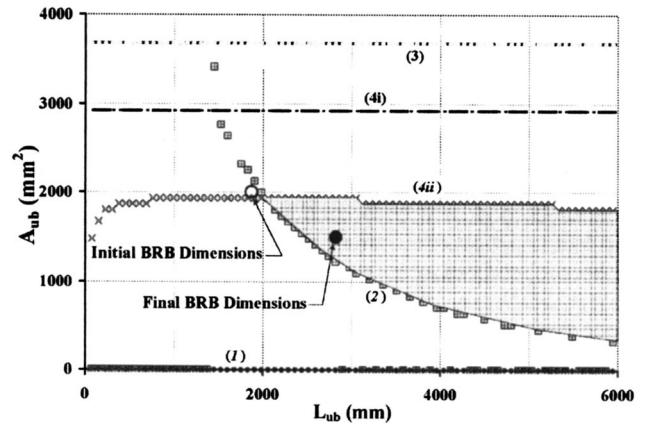


Fig. 4. Example graphical design procedure

3,980 kN, respectively. The dynamic amplification factors, R_{db} and R_{dL} , are taken as 1.56 and 1.87, respectively, and have been calculated using concepts presented in Pollino and Bruneau (2004). The BRBs are assumed to be implemented vertically and have a steel core with a yield stress of 235 MPa [LYP 235, Nakashima (1995)].

Since the fixed-base period of vibration, T_o , is greater than T_s , the retrofitted bridge will have an effective period of vibration in the long period range ($>T_s$). Therefore, the elastic spectral acceleration for the fixed-base system can be determined by Eq. (31). With the horizontal and vertical reactive weights assumed equal, Eq. (32) is evaluated as

$$\frac{1.0 \cdot 0.5g \cdot s}{0.8 \cdot 0.74s \cdot g} \geq \frac{1}{2} \cdot \frac{1,730 \text{ kN}}{1,730 \text{ kN}} \cdot \frac{1}{4} = 0.84 > 0.125 \quad (34)$$

thus indicating that uplift and rocking motion will occur.

The BRB area is initially sized to satisfy the effective lateral base shear limit [Eq. (26)], resulting in a value of 2,000 mm². The BRB effective length (L_{ub}) is initially determined from Eq. (33), resulting in a length of 1,900 mm. Initial design constraints are then calculated (design iteration 0); results are shown in Table 1. Also, Fig. 4 shows the graphical design method for the example considered. Each constraint boundary line (1–4) is shown and the design solution space is shaded. The initially selected brace dimensions are marked and shown to lie outside the solution space.

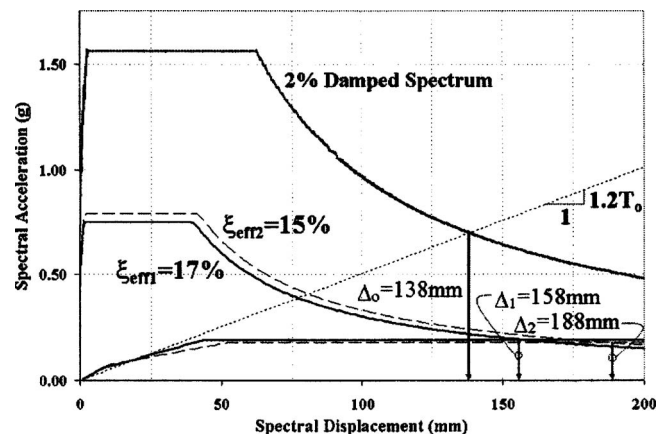


Fig. 5. Example capacity spectrum analysis iterations

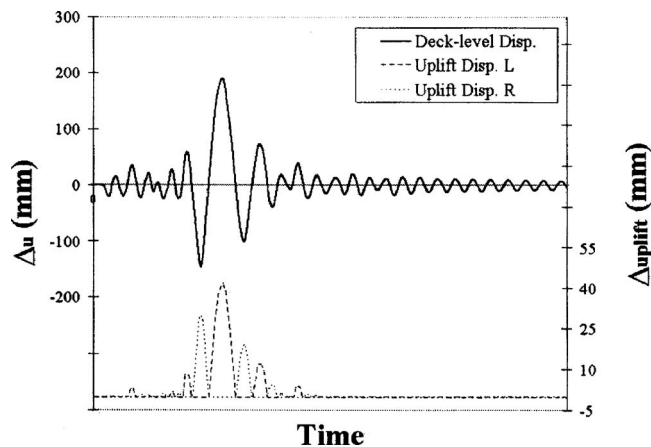


Fig. 6. Deck-level and uplifting displacement results of example TH analysis

Method 2 is now used to more accurately predict the maximum system displacement and the uplifting displacement. As discussed previously, this method uses spectral capacity (pushover) and demand curves to predict system response. System response for each design iteration is shown graphically in Fig. 5. The initial estimate of maximum system displacement (implicit in Step 6) is shown in the figure as Δ_o . The first iteration using analysis Method 2, based on the initial brace dimensions from the initial analysis, results in a maximum system displacement of 158 mm and an uplifting displacement [Eq. (22)] of 32.9 mm. The impact velocity is predicted using the system's pseudovelocity.

As seen in Table 1, the values of uplifting displacement and impact velocity do not satisfy their respective constraints. Following the guidance provided in the constraints section of this paper to satisfy these two constraints, L_{ub} is increased to satisfy the brace ductility demand limit, and A_{ub} is decreased in this case to increase the allowable impact velocity ($v_{o,allow}$) to satisfy the pier leg demand limit. The graphical design method (Fig. 4) shows how the brace dimensions need to be modified to satisfy the constraints. For the second iteration, the BRB cross-sectional area (A_{ub}) is taken as 1,500 mm² and effective length (L_{ub}) as 2,750 mm. The two constraints from Step 7 are recalculated along with each response prediction and given in Table 1. Finally, after reanalyzing using Method 2 and the above properties, all design

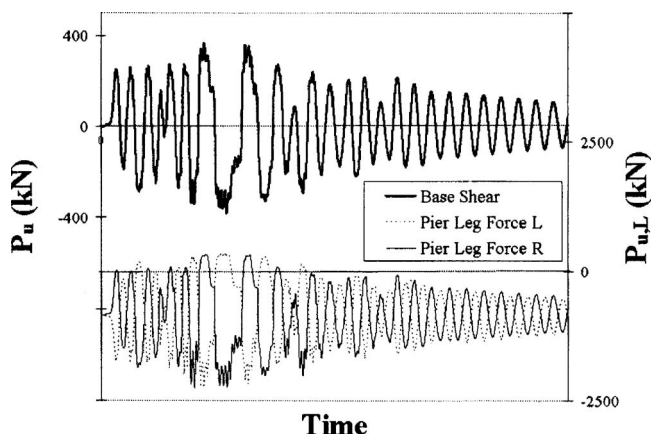


Fig. 7. Base shear and leg force results of example TH analysis

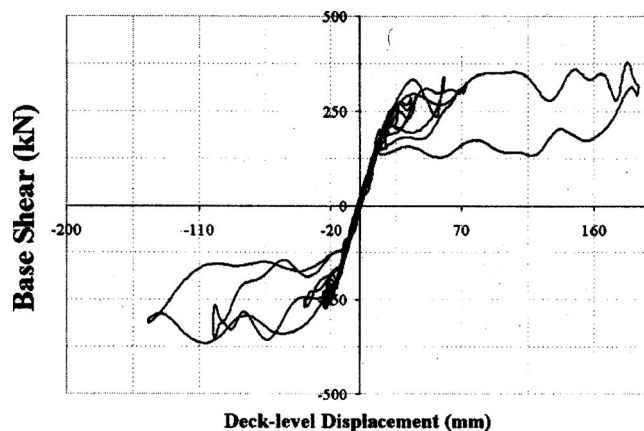


Fig. 8. Pier hysteretic behavior during example TH analysis

values are found to satisfy the specified design constraints, and the design point in Fig. 4 is shown to lie within the design solution space.

To illustrate the effectiveness of the proposed design procedure, a nonlinear inelastic time history analysis is performed to calculate the "actual" response of the retrofitted system. Details of the analytical model and earthquake loading used are identical to those used for the parametric study and are discussed in the following section. Results are shown in Table 1, confirming that all design constraints are satisfied. The displacement results ($\Delta_u, \Delta_{uplift}$) are shown to be predicted accurately; but the force response values, especially the pier leg axial force (P_{uL}), may possibly be predicted as overly conservative and a combination rule may need to be applied, as noted previously.

Results for selected response quantities are given in Figs. 6 and 7 and the resulting pier hysteretic behavior is given in Fig. 8. Fluctuation of the base shear shown in Fig. 8, compared to the idealized flag-shaped hysteretic behavior of the controlled rocking system, is due to the excitation of vertical modes of vibration of the truss during pier uplift and is accounted for by the dynamic amplification factor, R_{dv} , as discussed previously. The deck-level displacement results (Fig. 6) show the system returning to its original undeformed position at the end of the excitation due to the self-centering ability of the system.

Parametric Study to Assess Design Response Values

The design process described earlier relies on the prediction of response values needed for the design of the controlled rocking approach (displacement, velocity, base shear, and pier leg forces of the system) to ensure that they meet the specified design constraints. A parametric study using nonlinear inelastic time history analysis serves here to assess the accuracy of the predicted design response values. The analyses were performed with the structural

Table 2. Representative Pier Properties

h/d	h (m)	d (m)	w (kN)	k_o (kN/mm)	T_o (s)	k_L (kN/mm)	R_{dv}	R_{dL}
4	29.26	7.32	1730	12.5	0.74	212	1.56	1.87
3	21.95	7.32	1730	23.1	0.55	282	1.8	1.91
2	14.63	7.32	1730	47.5	0.38	423	1.93	1.93

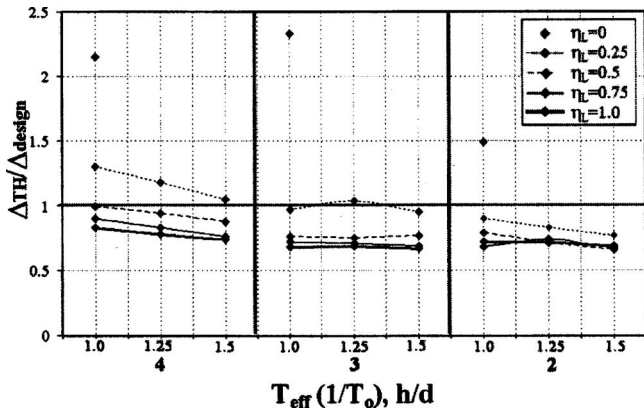


Fig. 9. Normalized deck-level displacement results (Method 1)

analysis program SAP2000 version 7.40 (Wilson 2000) with an equivalent viscous damping of 2% assigned to each mode.

The parameters here include a set of pier properties, given in Table 2; local strength ratios, η_L , varied from zero (elastic rocking) to the point at which the self-centering ability is lost ($\eta_L=1.0$); and an effective period of vibration characterized by Eq. (15) with k_{eff} defined by Eq. (16).

Results are presented for aspect ratios of 4, 3, and 2; local strength ratios (η_L) of 0, 0.25, 0.5, 0.75, and 1.0; and three effective periods of vibration ($\sim 1.0T_o$, $1.25T_o$, and $1.5T_o$), where T_o is the pier's fixed base period of vibration, and are given in Table 2. In the case of $\eta_L=0$, only the initial period of vibration of the pier is relevant since no BRB is used.

Earthquake Loading

Spectra-compatible ground acceleration time histories used for the dynamic analyses are generated using Target Acceleration Spectra Compatible Time Histories (TARSCTHS) software, which was developed by the Engineering Seismology Laboratory (ESL) at the University at Buffalo and is the implementation of the method described in Deodatis (1996). Synthetic ground motions were generated by TARSCTHS matching an elastic response spectral shape defined by NCHRP 12-49 (ATC/MCEER 2003). A design 1 s spectral acceleration values (S_{D1}) of 0.5g is considered here, with the design short period spectral acceleration value (S_{DS}) assumed equal to 2.5 times S_{D1} . This results in a characteristic period, T_s , of 0.4 s, typical of a rock site. Seven randomly generated synthetic motions were produced with a duration of 15 s.

Analytical Model

For the proposed controlled rocking bridge pier system considered here, the piers are excited solely in the horizontal direction. Each pier is assumed to carry an equal inertia mass both vertically and horizontally. A 2D model of each representative truss pier is used with half of the mass applied to each of the top two nodes of the truss. The pier itself is modeled with its elastic properties, and all nonlinear action is modeled to occur at the foundation interface. A compression-only "gap" element and a displacement-based hysteretic element are placed in parallel across the anchorage interface, at the base of each pier leg, to model the rocking behavior. The gap elements represent the foundation with no tensile capacity and a large linear-elastic stiffness in compression. The hysteretic element is based on the model proposed by Wen

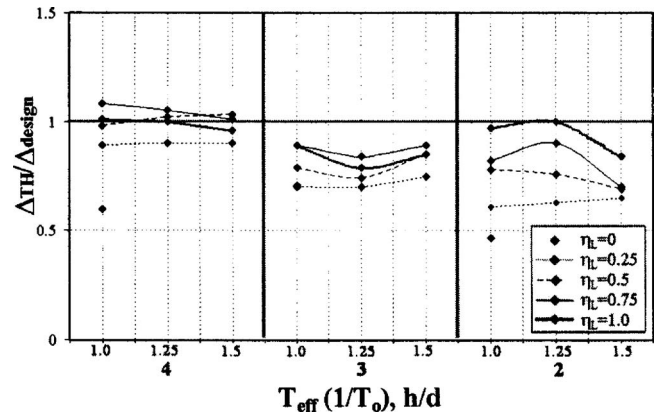


Fig. 10. Normalized deck-level displacement results (Method 2)

(1976). Restraints are provided at the anchorage level that prevent movement in the horizontal direction (thus assuming that sliding is prevented), but provide no resistance to vertical movements.

Results and Discussion

The mean result of the seven synthetic ground motions is shown for each case considered. A total of 39 cases and 273 analysis were performed. Results are presented for deck-level displacements (Δ_d), maximum base shear ($P_{u,TH}$), and maximum pier leg axial force ($P_{uL,TH}$) normalized by their respective design response value, for each system parameter considered. Displacement design response values are determined using analysis methods 1 and 2. The base shear (P_u) and pier leg axial force (P_{uL}) design response values are given by Eqs. (25) and (28), respectively.

Deck-Level Displacements

Results of the normalized deck-level displacements are shown in Figs. 9 and 10 for methods 1 and 2, respectively. As can be seen in the figures, Method 2 is able to more accurately predict displacements for all ranges of parameters considered here. Method 1 works well for systems with $\eta_L > 0.5$, but for smaller values of η_L the method tends to underpredict the maximum displacements.

The primary difference between the two methods is seen at small values of the local strength ratio, η_L , where large increases

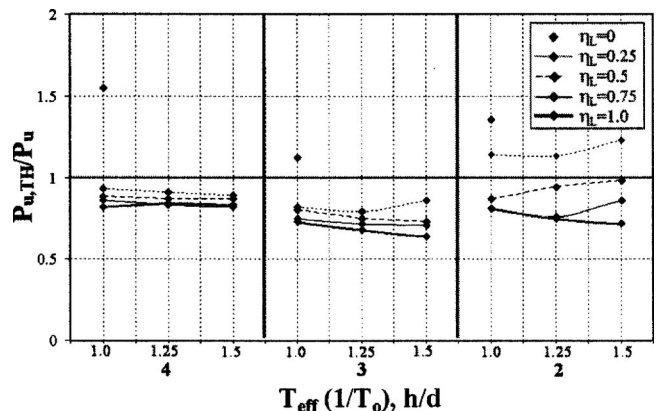


Fig. 11. Normalized base shear results

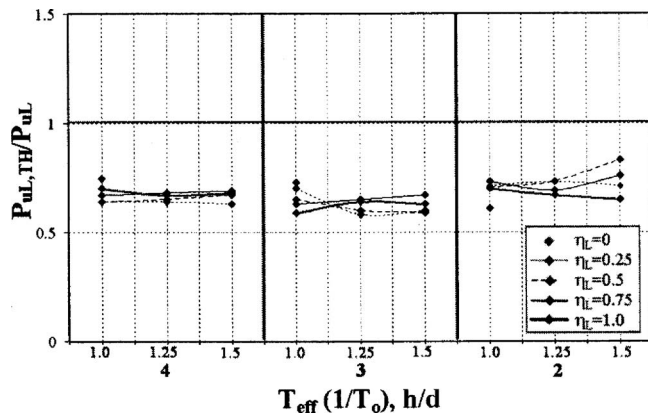


Fig. 12. Normalized pier leg axial force results

in displacements are predicted by Method 2 due to the decrease in system strength and energy dissipation with small BRB areas. Method 1 underpredicts displacements (for smaller values of η_L), as seen in Fig. 9, especially for the case of the bilinear elastic rocking system ($\eta_L=0$). While Method 2 does not necessarily provide the exact solution, it captures trends in flag-shaped behavior that have significant influence on response. These trends include system strength, initial stiffness, postelastic stiffness, and energy dissipating ability, while Method 1 is completely dependent on an effective initial elastic stiffness.

Base Shear Results

The time history analysis base shear results, $P_{u,TH}$, normalized by its design response value, P_u (Fig. 11), show that the prediction of the ultimate base shear, including dynamic effects, is conservative for $\eta_L \geq 0.25$, except for a pier aspect ratio of 2 with $\eta_L=0.25$. It is also unconservative for the case of bilinear, elastic rocking (i.e., $\eta_L=0$).

Pier Leg Force Results

The time history results of forces developed in the pier legs, $P_{uL,TH}$, normalized to its design response value, P_{uL} defined by Eq. (28), are shown in Fig. 12. The conservative assumptions made in the derivation of Eq. (28) (namely the in-phase response of all dynamic effects during impact and uplift), resulted in conservative estimates of the pier leg demands in all cases considered here. Conservative predictions of the demands to the pier legs are key, given that the pier legs resist the pier's gravity load.

Conclusions

This paper investigated a seismic retrofit technique that allows bridge steel truss piers to uplift and rock on their foundation, with passive energy dissipation devices (BRBs) used to control the rocking response while providing additional energy dissipation. This controlled rocking system has an inherent restoring force that can be designed to provide pier self-centering and leave the bridge with no residual displacements following an earthquake.

The hysteretic behavior of the controlled rocking system with displacement-based, steel yielding devices (BRBs) implemented at the anchorage location and the change in the behavior during cyclic loading (second-cycle response) have been presented.

A capacity-based design procedure for the controlled rocking approach is proposed. A set of design constraints is established to achieve ductile seismic performance, which includes pier drift, ductility demands on the BRB, self-centering, and maximum developed force limits. Methods to determine design response values (displacements, velocity, forces) are also presented. A design example is provided to show the key steps in the design procedure. A series of iterations is performed and a set of BRB properties selected to satisfy all design constraints. Time history analysis is performed, using the example's pier properties and the final selected brace dimensions, and the response is shown to satisfy all design constraints.

The proposed methods for determining design response values are evaluated through a parametric study based on nonlinear inelastic time history analysis. The analysis results are presented as normalized to the design response values. Results relevant for capacity design (base shear and pier leg forces) were found to be conservative in almost all cases considered.

Acknowledgments

This research was supported in part by the Federal Highway Administration under Contract No. DTFH61-98-C-00094 to the Multidisciplinary Center for Earthquake Engineering Research. However, any opinions, findings, conclusions, and recommendations presented in this paper are those of the writers and do not necessarily reflect the views of the sponsors.

References

- ATC/MCEER. (2003). "NCHRP 12-49 recommended LRFD guidelines for the seismic design of highway bridges. I: Specification." ATC/MCEER Joint Venture, Buffalo, N.Y.
- Berman, J. W., and Bruneau, M. (2005). "Approaches for the seismic retrofit of braced steel bridge piers and proof-of-concept testing of an eccentrically braced frame with tubular link." *Technical Rep. MCEER-05-0004*, Multidisciplinary Center for Earthquake Engineering Research, State Univ. of New York at Buffalo, Buffalo, N.Y.
- Black, C., Makris, N., and Aiken, I. (2002). "Component testing, stability analysis and characterization of buckling-restrained unbonded braces." *Rep. No. EERC 2002-08*, Earthquake Engineering Research Center, College of Engineering, Univ. of California, Berkeley, Calif.
- Deodatis, G. (1996). "Nonstationary stochastic vector processes: Seismic ground motion applications." *Probab. Eng. Mech.*, 11(3), 149–167.
- Dowdell, D., and Hamersley, B. (2000). "Lions' Gate Bridge North Approach: Seismic retrofit." *Behaviour of Steel Structures in Seismic Areas: Proc., 3rd Int. Conf.: STESSA 2000*, Balkema, The Netherlands, 319–326.
- Federal Emergency Management Agency (FEMA). (1997). *FEMA 274 NEHRP commentary on the guidelines for the seismic rehabilitation of buildings*, Building Seismic Safety Council, Washington, D.C.
- Federal Emergency Management Agency (FEMA). (2000). *FEMA 356 prestandard and commentary for the seismic rehabilitation of buildings*, Building Seismic Safety Council, Washington, D.C.
- Hasegawa, H., Takeuchi, T., Nakata, Y., Iwata, M., Yamada, S., and Akiyama, H. (1999). "Experimental study on dynamic behavior of unbonded braces." *J. Architectural and Building Sci.*, 114(1448), 103–106.
- Housner, G. (1963). "The behavior of inverted pendulum structures during earthquakes." *Bull. Seismol. Soc. Am.*, 53(2), 403–417.
- Ingham, T., Rodriguez, S., Nadar, M., Taucer, F., and Seim, C. (1995).

- "Seismic retrofit of the Golden Gate Bridge." *Proc., National Seismic Conf. on Bridges and Highways: Progress in Research and Practice*, Federal Highway Administration, Washington, D.C.
- Iwata, M., Kato, T., and Wada, A. (2000). "Buckling-restrained braces as hysteretic dampers." *Behaviour of steel structures in seismic area, STESSA 2000*, Balkema, The Netherlands, 33–38.
- Jones, M., Holloway, L., Toan, V., and Hinman, J. (1997). "Seismic retrofit of the 1927 Carquinez Bridge by a displacement capacity approach." *Proc., 2nd National Seismic Conf. on Bridges and Highways: Progress in Research and Practice*, Federal Highway Administration, Washington, D.C.
- Kelley, J., and Tsztoo, D. (1977). "Earthquake simulation testing of a stepping frame with energy-absorbing devices." *Rep. No. EERC 77-17*, Earthquake Engineering Research Center, College of Engineering, Univ. of California, Berkeley, Calif.
- Lee, K., and Bruneau, M. (2004). "Seismic vulnerability evaluation of axially loaded steel built-up laced members." *Technical Rep. MCEER-04-0007*, Multidisciplinary Center for Earthquake Engineering Research, State Univ. of New York at Buffalo, Buffalo, N.Y.
- Mander, J., and Cheng, C. (1997). "Seismic resistance of bridge piers based on damage avoidance design." *Technical Rep. NCEER-97-0014*, National Center for Earthquake Engineering Research, State Univ. of New York at Buffalo, Buffalo, N.Y.
- Meek, J. W. (1975). "Effects of foundation tipping on dynamic response." *J. Struct. Div.*, 101(7), 1297–1311.
- Midorikawa, M., Azuhata, T., Ishihara, T., and Wada, A. (2003). "Shaking table tests on rocking structural systems installed yielding base plates in steel frames." *Behaviour of steel structures in seismic areas, STESSA 2003*, Balkema, The Netherlands, 449–454.
- Nakashima, M. (1995). "Strain-hardening behavior of shear panel made of low-yield steel. I: Test." *J. Struct. Eng.*, 121(12), 1742–1749.
- Newmark, N., and Hall, W. (1982). *Earthquake spectra and design*, Earthquake Engineering Research Institute, Oakland, Calif.
- Pollino, M., and Bruneau, M. (2004). "Seismic retrofit of bridge steel truss piers using a controlled rocking approach." *Technical Rep. MCEER-04-0011*, Multidisciplinary Center for Earthquake Engineering Research, State Univ. of New York at Buffalo, Buffalo, N.Y.
- Priestley, M. J. N., Evison, R. J., and Carr, A. J. (1978). "Seismic response of structures free to rock on their foundations." *New Zealand Nat. Soc. Earthquake Eng. Bull.*, 11(3), 141–150.
- Priestley, M. J. N., Seible, F., and Calvi, G. M. (1996). *Seismic design and retrofit of bridges*, Wiley, New York.
- Ritchie, P., Kaulh, N., and Kulicki, J. (1999). "Critical seismic issues for existing steel bridges." *Technical Rep. MCEER-99-0013*, Multidisciplinary Center for Earthquake Engineering Research, State Univ. of New York at Buffalo, Buffalo, N.Y.
- Sarraf, M., and Bruneau, M. (1998). "Ductile seismic retrofit of steel deck-truss bridges. II: Design applications." *J. Struct. Eng.*, 124(11), 1263–1271.
- Toranzo, L. A., Carr, A. J., and Restrepo, J. I. (2001). "Displacement based design of rocking walls incorporating hysteretic energy dissipators." *7th Int. Seminar on Seismic Isolation, Passive Energy Dissipation and Active Control of Vibrations of Structure*.
- Wada, A., Saeki, E., Takeuch, T., and Watanabe, A. (1989). "Development of unbonded brace" *Column (A Nippon Steel Publication)*, No. 115 1989.12.
- Watanabe, A., Hitomoi, Y., Saeki, E., Wada, A., and Fujimoto, M. (1988). "Properties of brace encased in buckling-restraining concrete and steel tube." *Proc., 9th World Conf. on Earthquake Engineering*, Vol. IV, 719–724.
- Watanabe, A., and Nakamura, H. (1992). "Study on the behavior of buildings using steel with low yield point." *Proc., 10th World Conf. on Earthquake Engineering*, Balkema, Rotterdam, The Netherlands, 4465–4468.
- Wen, Y.-K. (1976). "Method for random vibration of hysteretic systems." *J. Engrg. Mech. Div.* 102(2), 249–263.
- Wilson, E. (2000). *Three-dimensional static and dynamic analysis of structures*, Computers and Structures, Inc., Berkeley, Calif.